Journal of Materials Chemistry A

Accepted Manuscript

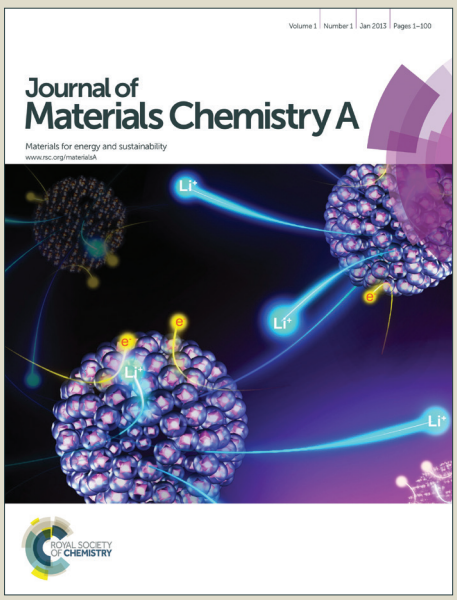

ROYAL SOCIETY OF CHEMISTRY

www.rsc.org/materialsA

Effect of Processing Additive on Morphology and Charge Extraction in Bulk-Heterojunction Solar Cells

Dong Hwan Wang, *[a] Pierre-Olivier Morin,[b] Chang-Lyoul Lee,[c] Aung Ko Ko Kyaw,[d,e] Mario Leclerc[b] and Alan J. Heeger *[e]

Received (in XXX, XXX) Xth XXXXXXXXX 200X, Accepted Xth XXXXXXXXX 200X
First published on the web Xth XXXXXXXXX 200X
DOI: 10.1039/b000000x

The effects of the 1,8-diiodooctane (DIO) processing additive on the nanomorphology, charge generation, and charge transport in the PBnDT-FTAZ/$PC_{70}BM$ BHJ solar cells are demonstrated. The optimized nanoscale donor-acceptor morphology is achieved with 3% DIO processing additive in the BHJ film. The BHJ film with 3% DIO exhibits efficient charge generation as indicated by the decreased PL and the associated lifetime compared to the BHJ film without DIO. The balanced charge transport decreased series resistance and balanced hole and electron mobility is also observed in the device fabricated with 3% DIO. Because of the efficient charge extraction, J_{SC} and PCE of the devices are increased from 3.7 mA/cm2 and 1.9% to 13.7 mA/cm^2 and 7%, respectively. In summary, optimized fabrication with DIO as a processing additive improves the morphology, faster charge generation, and balanced charge transport in the PBnDT-FTAZ:$PC_{70}BM$ BHJ film, which leads to high performance BHJ solar cells.

Introduction

Bulk-heterojunction (BHJ) solar cells based on organic donor and fullerene derivative acceptor blends with a phase-separated interpenetrating network structure have been developed with good progress during the past decade.[1-10] Compared to inorganic solar cells, the BHJ solar cells exhibit several advantages; specifically low cost soluton processing, light weight, and flexibility.[11-13] In order to improve the device performance and the nanomorphology of the BHJ active layer, various fabrication procedures have been carried out; thermal and solvent annealing process,[14-17] layer-evolved heterojunction for spontaneous interdiffusion,[18-20] and insertion of interlayers for efficient transport.[21-24] The most successful approach to improving the morphology is the addition of a processing additive (even at small concentrations, 0.4% ~ 5%)[25-29] and thereby enhance the power conversion efficiency (PCE). The optimized use of processing additives has resulted in remarkable increases of the photoconductivity, carrier mobility, and carrier life time.[26,30]

We recently synthesized the promising polymer; incorporating benzodithiophene (BnDT) as a donor and fluorinated 2-alkyl-benzo[d][1,2,3]triazoles (FTAZ) as a acceptor (see Figure. 1(a) for material structures). It is known that the substituted fluorine increased the electron-withdrawing characteristics which leads to a larger open circuit voltages for both polymers and small molecule donors.[31-32] Moreover, PBnDT-FTAZ with band-gap of 1.94 eV is a candidate polymer for use in tandem cells; i.e. two sub-cells stacked in series with BHJ films absorbing different fraction of the solar spectra. (See Supporting Information). The spectrum PBnDT-FTAZ can be made orthogonal to narrow band-gap materials. Also, the large difference between the highest occupied molecular orbital (HOMO) and lowest unoccupied molecular orbital (LUMO) provides the possibility of increased open-circuit voltage compared to the widely known poly(3-hexylthiophene) (P3HT) (~ 0.6 V).

In this research, we report the effect of processing additive for improved morphology, efficient charge generation, and charge transport in the PBnDT-FTAZ:[6,6]-phenyl C_{70}-butyric acid methyl ester ($PC_{70}BM$) BHJ solar cells processed from solution. From the AFM analysis of the morphology, the optimized additive (3% DIO) improves the nanoscale phase separation compared to cells fabricated without additive, or with use of 3% CN, and 3% DIH. In addition, the BHJ film with optimized processing additive exhibits efficient charge generation as evidenced by the decreased photoluminescence (PL) and the associated lifetime. The processing additive also leads to increased charge transport and decreased series resistance by means of the balanced hole and electron charge carrier mobility.

Experimental

Synthesis of PBnDt-FTAZ: A 20 mL microwave vial was charged with 0.1320 g (0.1490 mmol) of 2,6-bis(trimethyltin)-4,8-(3-hexylundecyl)benzo[1,2b:4,5-b']dithiophene, 0.09675 g (0.1499 mmol) of 4,7-bis(5-bromothiophen-2-yl)-2-(2-butyloctyl)-2H-benzo[d][1,2,3]triazole, 0.0027g (2%) of $Pd_2(dba)_3$, 0.0073g (16%) of P(o-tolyl)$_3$, and 3.7 mL (0.04 M) of degassed toluene. The reaction mixture was vigorously stirred for 66h at 120 °C in an oil-bath. The reaction was cooled at room temperature and the polymer was precipitated in methanol/water (9:1), filtered through 0.45 mm nylon filter and washed on Soxhlet apparatus with acetone, hexanes and then chloroform. The chloroform fraction was reduced to 20 - 30 mL and precipitated in methanol/water (9:1), filtered through 0.45 µm nylon filter and air-dried to give 138 mg of the desired polymer (91 % yield).

Fabrication of solar cells: The ITO-coated glass substrates were first cleaned by ultrasonic agitation in detergent, deionized water, acetone and isopropanol sequentially, then the UV ozone treatment was followed by 15 min. The hole transport layer of commercial PEDOT:PSS (AI 4083) was spin-coated at 5000 rpm for 40 s to the film thickness of ~35 nm. The BHJ active layers (ca. ~100 nm) were spin-cast in a N_2 filled glove box from the solution of PBnDt-FTAZ:$PC_{70}BM$ (1:2 weight ratio) in chlorobenzene (CB) without and with 3 v/v% DIO, with the

overall concentration of 36 mg/mL. $PC_{70}BM$ were purchased from Solenne BV. The prepared solutions were heating at 60°C during overnight. The BHJ was coated by PTFE filter of 0.2 µm with a thickness from 60 nm to 200 nm depending on 900 rpm to 3000 rpm The films were annealed at 70°C for 10 min to evaporate residual solvent. Finally, Ca/Al (20 nm/100 nm) were thermally deposited sequentially under 4×10^{-6} Torr by evaporator.

Characterization of BHJ solar cells: The light source was calibrated by using silicon reference cells with an AM 1.5 Global solar simulator (from an intensity of 100 mW/cm^2). The *J-V* characteristics of the solar cells were measured by a Keithley 236 source unit. All the cell areas are 11.76 mm^2 as determined by the aperture to accurate measurement of PCE parameters. The EQE was measured using a QE measurement system (PV measurements, Inc.) after monochromatic power calibration to confirm the J_{SC} value.

Time-Correlated Single Photon Counting (TCSPC): Time-Correlated Single Photon Counting (TCSPC) was performed to measure the exciton lifetimes. The second harmonic (SHG = 400 nm) of a tunable Ti:sapphire laser (Mira900, Coherent) with an ~150 fs pulse width and 76 MHz repetition rate was used as the excitation source. The PL emission was resolved spectrally using some collection optics and a monochromater (SP-2150i, Acton). The TCSPC module (PicoHarp, PicoQuant) with a MCP-PMT (R3809U-59, Hamamatsu) was used for ultrafast detection. The total instrumental response function (IRF) for PL decay was less than 140 ps and the temporal time resolution was less than 10 ps. Deconvolution of the actual PL decay and IRF was performed by using fitting software (FlouFit, PicoQuant) to deduce the time constant associated with each exponential decay.

Other characterization methods: AFM images and roughness analysis were carried out with Asylum MFP3D. The absorption of BHJ films was measured by UV-vis-NIR spectrophotometer system (PerkinElmer Lambda 950) in transmittance mode.

Results and discussion

Property of PBnDT-FTAZ material and device performances of BHJ solar cells

The appropriate time of each process step is a critical factor for cost-effective fabrication and performance stability. Even though the PBnDT-FTAZ:PCBM BHJ is soluble for 1,2,4-trichlorobenzene (TCB), and the device operates well according to previous report[33], the coated BHJ active layer needs 12 hours of residual solvent drying time because of the high boiling point of TCB (~ 214.4°C) compared to chlorobenzene (CB) (~131°C). Here, we use CB as the solvent, and a drying time of BHJ film is reduced to approximately 10 min.

The molecular structure of PBnDT-FTAZ, and $PC_{70}BM$, normalized UV-vis absorption spectra of PBnDT-FTAZ, the device structure and the energy levels of the components used in the devices are shown in Figures 1(a), (b), and (c), respectively. The synthesis steps and characterization of the PBnDT-FTAZ polymer are described in detail in the Experimental Section and Supporting Information. The HOMO and LUMO of PBnDT-FTAZ polymer characterized from cyclic voltammetry measurement are -5.32 eV and -3.38 eV (see Figure S1), and the molecular weight is 73 kDa as shown in Table S1. Normalized UV-vis absorption spectra of PBnDT-FTAZ:$PC_{70}BM$ BHJ film (red curve) and transmittance of the ITO substrate (black curve) are displayed in Figure S2.

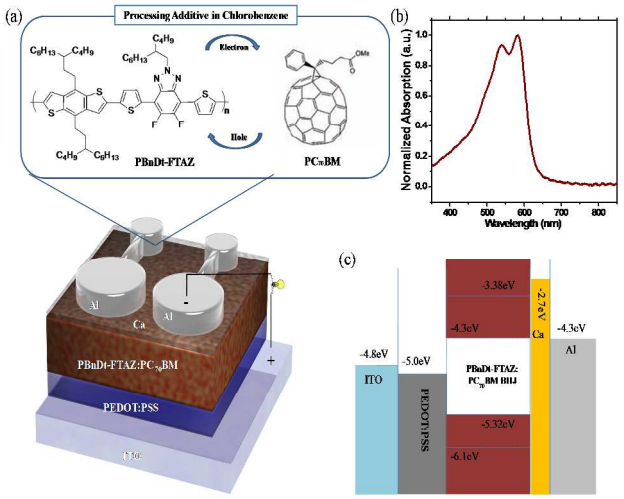

Figure 1. (a) The structure of the PBnDT-FTAZ:$PC_{70}BM$ BHJ solar cells. Inset shows the molecular structures of PBnDT-FTAZ and $PC_{70}BM$ (b) Normalized UV-vis absorption spectra of PBnDT-FTAZ (c) Energy level diagram of the components of the device.

The current density-voltage (*J-V*) characteristics of PBnDT-FTAZ:$PC_{70}BM$ BHJ solar cells with various processing additives (CB only, CB with 3% CN, CB with 3% DIH, CB with 3% DIO) (v/v) under AM 1.5G irradiation at 100 mW/cm^2 are shown in Figure 2(a).

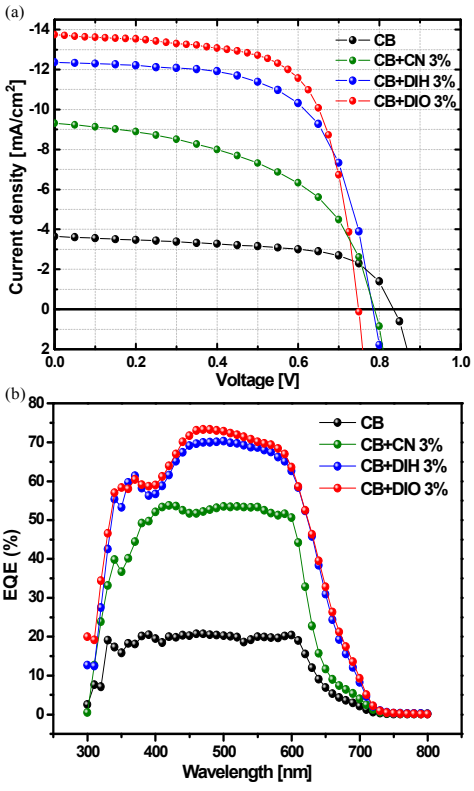

Figure 2. (a) *J-V* characteristics of the PBnDT-FTAZ:$PC_{70}BM$ BHJ devices fabricated without and with various processing additives under AM 1.5G irradiation at 100 mW/cm^2 (v/v) (b) EQE spectra of the photovoltaic devices fabricated without and with processing additives (D-A ratio of 1:2).

All the BHJ solar cells are optimized at a ratio of 1:2 (donor:acceptor) as shown in Figure S3 (a). The electrical parameters are summarized in Table 1. The device with only CB has PCE = 1.9% with a J_{SC} = 3.7 mA/cm^2, an V_{OC} = 0.84 V and a fill factor (FF) of 62%. When the processing additives, CN and DIH, are used with a ratio of 3% in CB, the V_{OC} decreases to 0.79 V and 0.78 V but J_{SC} increases to 9.3 mA/cm^2 and 12.4 mA/cm^2 and FF increases to 52% and 64%, respectively. Since the J_{SC} of BHJ solar cell is determined by the phase separation between donor and acceptor or as well as charge extraction, the enhanced film nanomorphology is one of the main reasons for increased J_{SC}. Therefore, the PCE improves to 3.8% and 6.2%, respectively. The device fabricated with DIO processing additive has significantly increased PCE = 7.0% with a J_{SC} = 13.7 mA/cm^2, V_{OC} = 0.75 V and FF = 68%. The increase of Voc (without additive) may be due to the increased surface roughness and rms (root mean square) which possibly influence the change of contact area or structural change at the PEDOT:PSS/BHJ active layer interface and wettability with metal electrode.[34] Hence, the performance of PBnDT-FTAZ:$PC_{70}BM$ BHJ solar cells is highly dependent on the optimization by the processing additive (See Figure S3 (b)). The external quantum efficiency (EQE) spectra obtained with cells fabricated with various processing additives are shown in Figure 2(b). The EQE value shows 20% for the device with only CB, while the maximum EQE exceeds 75 % near the wavelength range 450 nm and 500 nm for the device with the optimized DIO. Figure S3 (c) exhibits PCE ranges of the PBnDT-FTAZ:$PC_{70}BM$ BHJ device with DIO depending on various BHJ thicknesses from 60 nm to 200 nm. The BHJ is optimized at a thickness of 100 nm where the average PCE = 7%.

PBnDT-FTAZ:$PC_{70}BM$	V_{OC} [V]	J_{SC} [mA/cm^2]	FF [%]	PCE [%]
CB only	0.84	3.7	62	1.9
CB with CN 3%	0.79	9.3	52	3.8
CB with DIH 3%	0.78	12.4	64	6.2
CB with DIO 3%	0.75	13.7	68	7.0

Table 1. The electrical parameters of the PBnDT-FTAZ:$PC_{70}BM$ BHJ devices fabricated without and with various processing additive conditions (v/v).

Analysis of surface morphology, charge generation, and charge transport

The surface roughness and topography of the PBnDT-FTAZ:$PC_{70}BM$ BHJ films were investigated by atomic force microscopy (AFM) as shown in Figure 3. The BHJ film with only CB is composed of nano-sized aggregation regions with root mean square (rms) roughness of 16 nm. The BHJ films with processing additives of CN, DIH, and DIO exhibit smoother surface morphology with rms roughness of 8 nm, 3 nm, and 2 nm, respectively. As shown in Figure 3 (a), the BHJ film without additive displays micro-scale separation between donor and fullerene composite and exhibits significant roughness fluctuations, while the images of BHJ films with additive show homogeneous surface morphology and nanoscale phase separation because the additive affect the formation of a well-ordered BHJ nanomorphology without aggregation regions. The DIO additive has good solubility for both components which enables each phase to mix well in BHJ composite films. Thus, the processing additive plays an important role in improving the morphology of the BHJ films. The nanoscale phase separation between donor and acceptor (see Figure S4) is correlated to the increased J_{SC} and PCE of the devices. The device fabricated with DIO shows well defined surface nanomorphology from the two dimensional AFM height and phase images shown in Figure S4.

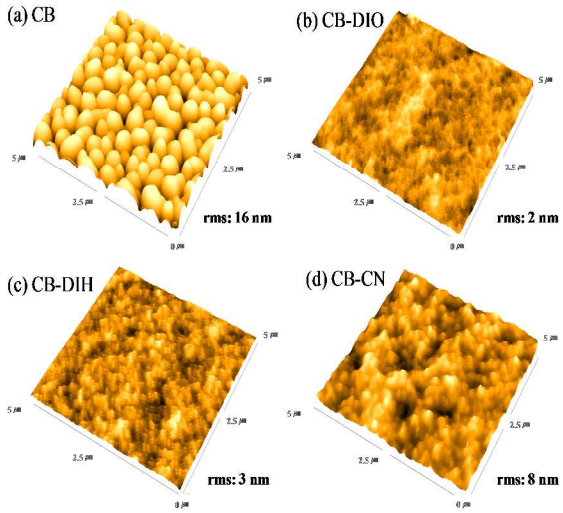

Figure 3. AFM images of PBnDT-FTAZ:$PC_{70}BM$ BHJ in (a) CB fabricated without processing additive and CB fabricated with processing additives of (b) DIO (3%) (c) DIH (3%) (d) CN (3%), respectively (v/v). The scan size is 5 × 5 μm for all height three-dimensional images (D-A ratio of 1:2).

The Figure 4(a) shows the PL intensity of pristine donor, BHJ without, and BHJ with DIO as a funtion of the wavelenght (nm). The reduced PL intensity of BHJ with DIO reveals increased charge separation in the film. Time-correlated single photon counting (TCSPC) was carried out to gain further insight into the relationship between exciton quenching efficiency of PBnDT-FTAZ:$PC_{70}BM$ film and photovoltaic device performance with and without DIO as shown in Figure 4(b). The PL decay profiles of PBnDT-FTAZ:$PC_{70}BM$ films with and without DIO were fitted well by a bi-exponential decay fitting[35-36], which suggests that the PL excitons decay of PBnDT-FTAZ took place through two relaxation pathways (See Table 2). The dominant term in the PL decay profiles, was reduced from 63% to 55% and lifetime decreased from 0.38 ns to 0.30 ns. Thus, the exciton quenching efficiency of PBnDT-FTAZ:$PC_{70}BM$ film increase by adding DIO, which is consistent with AFM and BHJ solar cell results.

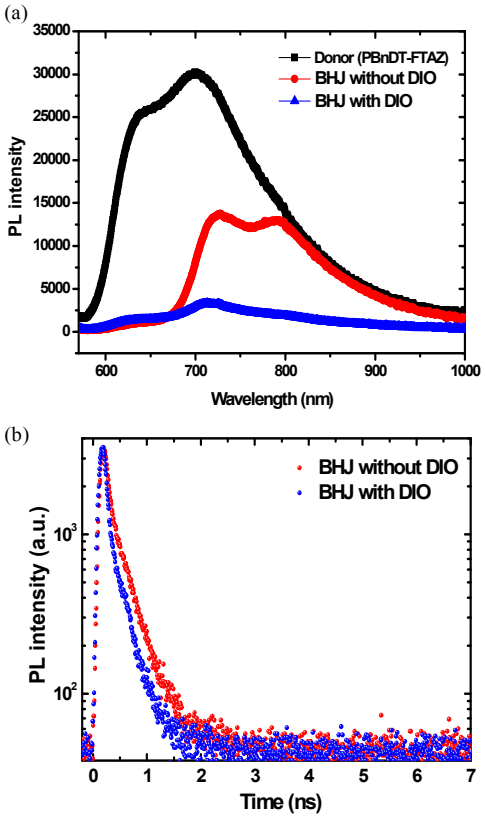

Figure 4. (a) PL intensity of pristine donor, BHJ without, and BHJ fabricated with DIO depending on wavelength (nm), and (b) PL decay profiles of PBnDT-FTAZ:$PC_{70}BM$ BHJ without and BHJ fabricated with DIO. The DIO content is 3% in CB (v/v) (D-A ratio of 1:2).

	τ_1[ns](f_1)	τ_2[ns](f_2)	τ_{avr}[ns][b]	χ^{2c}
Without DIO	0.38(0.63)	0.13(0.37)	0.29	1.255
With DIO	0.30(0.55)	0.07(0.45)	0.20	1.188

Table 2. PL lifetimes of PBnDT-FTAZ:$PC_{70}BM$ film fabricated without and with DIO[a].

The number of photogenerated charges extracted at electrode is determined by the competition between carrier sweep-out and recombination. Thus, the charge carrier mobility is a critical factor in the BHJ solar cells.[37] For this reason, we measured the dark current density-voltage (*J–V*) characteristics of single carrier cell to confirm the hole and electron mobilities of PBnDT-FTAZ:$PC_{70}BM$ BHJ film and then calculated the mobility values using the space-charge-limited current (SCLC) model described by the Mott-Gurney law which includes a small field dependent value;[37-40]

$$J = \frac{9}{8}\varepsilon_r\varepsilon_0\mu_0\frac{(V_{app}-V_{bi})^2}{L^3}\exp(\beta\sqrt{\frac{V_{app}-V_{bi}}{L}}) \quad (1)$$

where $\varepsilon_r\varepsilon_0$ is the dielectric permittivity (3.4) of the active layer, L is the thickness of the active layer (100 nm), V_{app} is applied voltage, V_{bi} is built-in voltage, μ_0 is the zero-field mobility and β is the field activation factor which is a free parameter for fitting, respectively. Figure 5 exhibits the *J-V* characteristics of the hole-only device without and with 3% DIO in the ITO/PEDOT:PSS /BHJ/MoO_x/Ag (Figure 5(a)) structure and the electron-only device of ITO/Al/BHJ/Ca/Al (Figure 5(b)) structure.

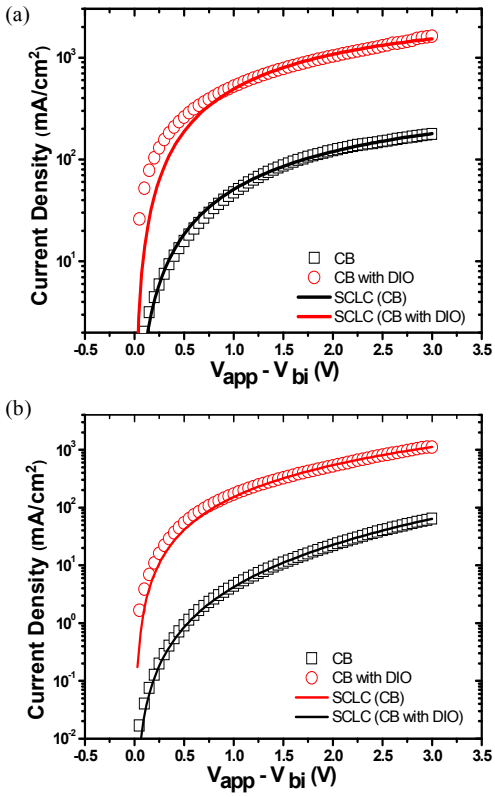

Figure 5. The effect of processing additive of DIO (3%) on charge transport properties. The dark *J-V* characteristics of (a) hole-only devices and (b) electron-only devices fabricated without and 3% DIO (shown in symbols). The solid lines represent the fitting using the SCLC model.

The solid lines of fitting graph from the experimental results reveals that the hole mobilities in the BHJ films are 5.3×10^{-4} cm^2/V-s and 6.2×10^{-3} cm^2/V-s for the BHJ film fabricated without and with 3% DIO, respectively. The increased hole mobility with DIO is consistent with our previous data of improved morphology with nanoscale percolated pathway by processing additive. Also, the electron mobility of the BHJ films fabricated without and with the use of 3% DIO exhibits large difference, 6.0×10^{-6} cm^2/V-s and 5.9×10^{-4} cm^2/V-s, respectively. The electron mobility decreases sharply without the use of the 3% DIO. Therefore, the hole and electron mobility are more nearly balanced in the BHJ film fabricated with 3% DIO in CB with decreased series resistance (R_s) from 10.3 Ωcm^2 to 1.6 Ωcm^2 and enhanced shunt resistance (R_{sh}) from 1.1 kΩcm^2 to 1.3 kΩcm^2. To confirm the device durability of BHJ film fabricated with DIO, we examined the device life time. Figure 6 displays

normalized PCE, J_{SC}, V_{OC} and FF of the device as a function of storage time after encapsulation in air. The device shows relatively good stability with slightly decreased J_{SC} and FF (~7%) after 100 hours, while the V_{OC} were stable.

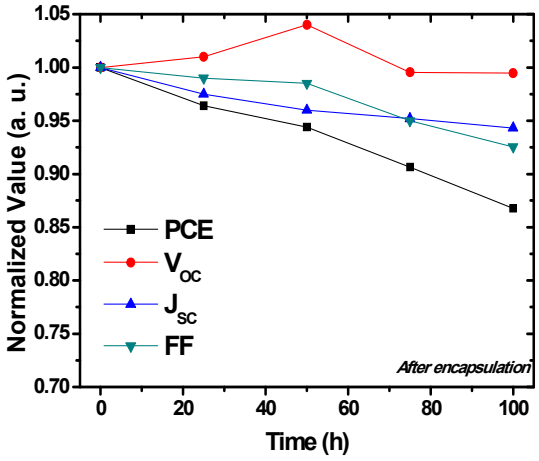

Figure 6. Normalized PCE, J_{SC}, V_{OC} and FF of the PBnDT-FTAZ:$PC_{70}BM$ BHJ device as a function of storage time after encapsulation in air.

Conclusions

In conclusion, we have been demonstrated PBnDT-FTAZ:$PC_{70}BM$ BHJ solar cells with PCE = 7 % using optimized processing additive of 3% DIO with enhanced J_{SC} and FF. Furthermore, the BHJ film fabricated with 3% DIO exhibits enhanced charge generation as evidenced by the decreased PL and the associated lifetime. The balanced charge transport and decreased series resistance are observed in the device with 3% DIO. Therefore, the optimized processing additive improves the morphology, enhanced charge generation, and yields nearly balanced charge transport in the PBnDT-FTAZ:$PC_{70}BM$ BHJ film, all of which lead to high performance BHJ solar cells.

Acknowledgements

This research was carried out at UCSB with support from the Air Force Office of Scientific Research, (AFOSR FA9550-11-1-0063), Dr. Charles Lee, Program Officer. This research was supported by Basic Science Research Program through the National Research Foundation of Korea (NRF) funded by the Ministry of Science, ICT & Future Planning (2014R1A1A1002419).

Notes and references

[a] *School of Integrative Engineering, Chung-Ang University, 221 Heukseok-dong, Dongjak-gu, Seoul 156-756, Republic of Korea; E-mail: king0401@cau.ac.kr*
[b] *Department of Chemistry Université Laval, Quebec City, QC, G1V 0A6, Canada*
[c] *Advanced Photonics Research Institute (APRI), Gwangju Institute of Science and Technology, 1 Oryong-dong, Buk-gu, Gwangju 500-712, Korea*
[d] *Institute of Materials Research and Engineering, Agency for Science Technology and Research (A*STAR), Singapore 117602, Republic of Singapore*
[e] *Center for Polymers and Organic Solids, University of California at Santa Barbara, Santa Barbara, California 93106-5090, USA; E-mail: ajhe1@physics.ucsb.edu*

†Electronic Supplementary Information (ESI) available: information of synthesized materials, device reproducibility, and AFM images. See DOI: 10.1039/b000000x/

1. G. Yu, J. Gao, J. C. Hummelen, F. Wudl, A. J. Heeger, *Science* 1995, **270**, 1789.
2. G. Li, V. Shrotriya, J. Huang, Y. Yao, T. Moriarty, K. Emery, Y. Yang, *Nat Mater.* 2005, **4**, 864.
3. J. Y. Kim, K. Lee, N. E. Coates, D. Moses, T.-Q. Nguyen, M. Dante, A. J. Heeger, *Science* 2007, **317**, 222.
4. S. H. Park, A. Roy, S. Beaupre, S. Cho, N. Coates, J. S. Moon, D. Moses, M. Leclerc, K. Lee, A. J. Heeger, *Nature Photonics* 2009, **3**, 297.
5. D. H. Wang, D. Y. Kim, K. W. Choi, J. H. Seo, S. H. Im, J. H. Park, O O. Park, A. J. Heeger, *Angew. Chem. Int. Ed.* 2011, **50**, 5519.
6. Y. Sun, G. C. Welch, W. L. Leong, C. J. Takacs, G. C. Bazan, A. J. Heeger, *Nat. Mater.* 2012, **11**, 44.
7. Z. He, C. Zhong, S. Su, M. Xu, H. Wu, Y. Cao, *Nat. Photonics* 2012, **6**, 591.
8. V. S. Gevaerts, A. Furlan, M. M. Wienk, M. Turbiez, R. A. J. Janssen, *Adv. Mater.* 2012, **24**, 2130.
9. J. H. Park, T.-W. Lee, B.-D. Chin, D. H. Wang, O O. Park, *Macromol Rapid Comm.* 2010, **31**, 2095.
10. T.-W. Lee, K.-G. Lim, D.-H. Kim, *Electron. Mater. Lett.* 2010, **6**, 41.
11. S. R. Forrest, *Nature* 2004, **428**, 911.
12. J. Peet, A. J. Heeger, G. C. Bazan, Acc. Chem. Res. 2009, **42**, 1700.
13. D. H. Wang, J. Seifter, J. H. Park, D.-G. Choi, A. J. Heeger, *Adv. Energy Mater.* 2012, **2**, 1319.
14. G. Li, V. Shrotriya, J. Huang, Y. Yao, T. Moriarty, K. Emery, Y. Yang, *Nat. Mater.* 2005, **4**, 864.
15. W. Ma, C. Yang, X. Gong, K. Lee, A. J. Heeger, *Adv. Funct. Mater.* 2005, **15**, 1617.
16. X. Yang, J. Loos, S. C. Veenstra, W. J. H. Verhees, M. M. Wienk, J. M. Kroon, M. A. J. Michels, R. A. J. Janssen, *Nano Lett.* 2005, **5**, 579.
17. G. Li, Y. Yao, H. Yang, V. Shrotriya, G. Yang, Y. Yang, *Adv. Funct. Mater.* 2007, **17**, 1636.
18. D. H. Wang, H. K. Lee, D.-G. Choi, J. H. Park, O O. Park, *Appl. Phys. Lett.* 2009, **95**, 043505.
19. J. S. Moon, C. J. Takacs, Y. Sun, A. J. Heeger, *Nano Lett.* 2011, **11**, 1036.
20. D. H. Wang, J. S. Moon, J. Seifter, J. Jo, J. H. Park, O. O. Park, A. J. Heeger, *Nano Lett.* 2011, **11**, 3163.
21. W. J. E. Beek, M. M. Wienk, R. A. J. Janssen, *Adv. Mater.* 2012, **16**, 1009.
22. Y. Sun, J. H. Seo, C.J. Takacs, J.Seifter, A. J. Heeger, *Adv. Mater.* 2012, **23**, 1679.
23. A. K. K. Kyaw, D. H. Wang, V. Gupta, W. L. Leong, L. Ke, G. C. Bazan, A. J. Heeger, *ACS Nano*, 2013, **7**, 4569.
24. D. H. Wang, J. K. Kim, J. H. Seo, I. Park, B. H. Hong, J. H. Park, A. J. Heeger *Angew. Chem. Int. Ed.* 2013, **52**, 2874.
25. J. Peet, J. Y. Kim, N. E. Coates, W. L. Ma, D. Moses, A. J. Heeger, G. C. Bazan, *Nat. Mater.* 2007, **6**, 497.
26. J. S. Moon, C. J. Takacs, S. Cho, R. C. Coffin, H. Kim, G. C. Bazan, A. J. Heeger, *Nano Lett.* 2010, **10**, 4005.
27. M.-S. Su, C.-Y. Kuo, M.-C. Yuan, U.S. Jeng, C.-J. Su, K.-H. Wei, *Adv. Mater.* 2011, **23**, 3315.
28. T.-Y. Chu, J. Lu, S. Beaupr, Y. Zhang, J.-R. Pouliot, S. Wakim, J. Zhou, M. Leclerc, Z. Li, J. Ding, Y. Tao, *J. Am. Chem. Soc.* 2011, **133**, 4250.
29. J. Jo, A. Pron, P. Berrouard, W. L. Leong, J. D. Yuen, J. S. Moon, M. Leclerc, A. J. Heeger, *Adv. Energy Mater.* 2012, **2**, 1397.
30. J. Peet, C. Soci, R. C. Coffin, T. Q. Nguyen, A. Mikhailovsky, D. Moses, G. C. Bazan, *Appl. Phys. Lett.* 2006, **89**, 252105.

31. H.-Y. Chen, J. Hou, S. Zhang, Y. Liang, G. Yang, Y. Yang, L. Yu, Y. Wu, G. Li, *Nat. Photonics* 2009, **3**, 649.
32. T. S. van der Poll, J. A. Love, T.-Q. Nguyen, G. C. Bazan, *Adv. Mater*. 2012, **24**, 3646.
33. S. C. Price, A. C. Stuart, L. Yang, H. Zhou, and Wei You, *J. Am. Chem. Soc*. 2011, **133**, 4625.
34. A. J. Moulé, K. Meerholz, *Adv. Mater*. 2008, **20**, 240.
35. H. Park, K. Y. Lee, W. Kim, H.-W. Shin, D. H. Wang, T. K. Ahn, J. H. Park, *ACS Appl. Mater. Interfaces*, 2013, **5**, 1612.
36. B. R. Lee, J.-w. Kim, D. Kang, D. W. Lee, S.-J. Ko, H. J. Lee, C.-L. Lee, J. Y. Kim, H. S. Shin, M. H. Song, *ACS Nano*, 2012, **6**, 2984.
37. P. N. Murgatroyd, *J. Phys. D: Appl. Phys*. 1970, **3**, 151.
38. S. M. Tuladhar, D. Poplavskyy, S. A. Choulis, J. R. Durrant, D. D. C. Bradley, J. Nelson, *Adv. Funct. Mater.* 2005, **15**, 1171.
39. V. D. Mihailetchi, H. X. Xie, B. de Boer, L. J. A. Koster, P. W. M. Blom, *Adv. Funct. Mater*. 2006, **16**, 699.
40. Z. He, C. Zhong, X. Huang, W.-Y. Wong, H. Wu, L.Chen, S. Su, Y. Cao, *Adv. Mater*. 2011, **23**, 4636.

Graphical Abstract

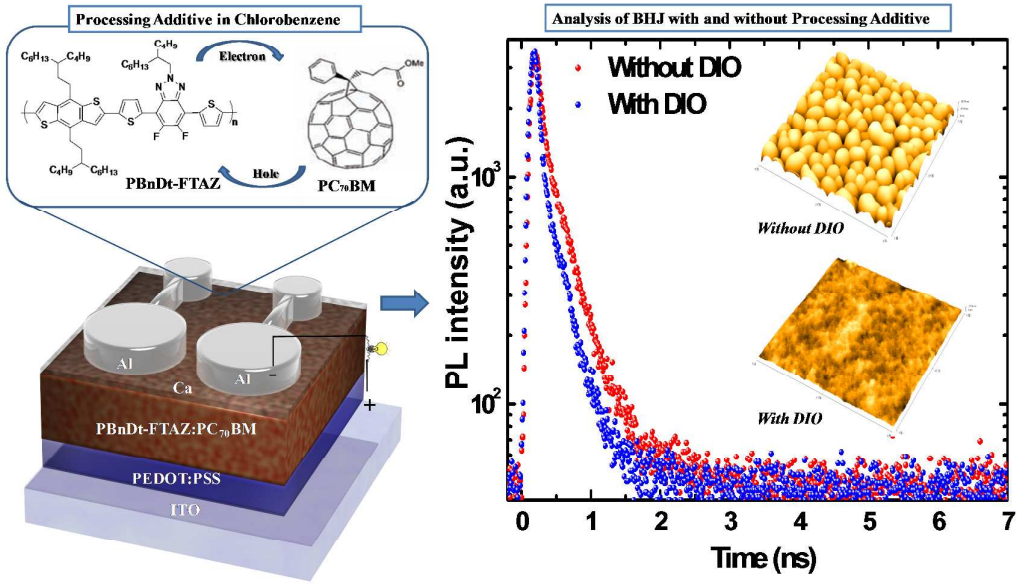

The PBnDT-FTAZ:$PC_{70}BM$ BHJ film fabricated with 3% DIO exhibits improved phase-separated morphology by AFM analysis and efficient charge generation as evidenced by decreased PL and the associated lifetime. The processing additive also leads to increased charge transport and decreased series resistance by means of the balanced hole and electron charge carrier mobility (by SCLC model).